Eur. Phys. J. B **44**, 137–143 (2005)
DOI: 10.1140/epjb/e2005-00109-4

THE EUROPEAN PHYSICAL JOURNAL B

A theoretical study of tunnelling conductance in ferromagnet/$PrOs_4Sb_{12}$ junctions

Guo-Ya Sun[a], Hai Lin, M.Y. Zeng, Yu-Hua Wen, and Chen-Xu Wu

Department of Physics, Xiamen University, Xiamen 361005, P.R. China

Received 29 September 2004 / Received in final form 9 January 2005
Published online 20 April 2005 –

Abstract. The tunnelling conductance spectra of ferromagnet/$PrOs_4Sb_{12}$ junctions are theoretically investigated by using the Blonder-Tinkham-Klapwijk theory. Three pairs of possible candidate for the pairing symmetry of superconducting energy gap of the recently discovered heavy-fermion unconventional superconductor $PrOs_4Sb_{12}$ are chosen for calculation. We have studied the spin-polarization effect on the conductance spectra, with respect to different strength of ferromagnetism of the ferromagnet and different strength of the interface barrier. Moreover, we have discussed the influence of nodal structures of the superconducting energy gap on the conductance spectra. Different features of the tunnelling conductance spectra were got, which may serve as useful theoretical comparisons for future experiments.

PACS. 74.50.+r Tunneling phenomena; point contacts, weak links, Josephson effects – 74.70.Tx Heavy-fermion superconductors – 74.20.Rp Pairing symmetries (other than s-wave)

1 Introduction

The recent discovery of superconductivity in cubic skutterudite $PrOs_4Sb_{12}$ (POS) has attracted considerable theoretical and experimental interests [1–9]. POS is a heavy fermion and nonmagnetic compound with unconventional superconductivity. It should be distinguished from the other unconventional superconductors in that it has a nonmagnetic ground state of the localized f electrons in the crystalline electric field [1,2]. On the other hand, it was indicated that there are multiple superconducting phases in this material, like in the uranium compounds as UPt_3 and superfluid ^{3}He. The heat capacity and the thermal expansion measurements both show jumps at around $T_{c1} = 1.85$ K and $T_{c2} = 1.75$ K in the absence of a magnetic field, indicating a possible novel feature of the superconducting state with double superconducting transition of POS, i.e., high temperature ($T < T_{c1}$) phase (A phase) and low temperature ($T < T_{c2}$) phase (B phase) [2–4]. Moreover, the thermal transport measurements in magnetic field rotated relative to the crystal axes demonstrate that a novel change in the symmetry of the superconducting gap function occurs deep inside the superconducting state, giving a clear indication that the gap function has six point nodes at [100] and that equivalent to [100] directions for the A phase ($H > 0.75$ T, $T \ll T_{c1}$), while in the B phase ($H < 0.75$ T, $T \ll T_{c2}$) the number of the point nodes decreases to four or two because of additional symmetry breaking [8,9]. The heavy fermion behavior of POS should be understood in light of the interaction of the electric quadrupole moments of Pr^{3+}, rather than local magnetic moments as in the other heavy fermion superconductors, with the conduction electrons [10,11]. POS may be the first superconductor whose Cooper pairs are mediated neither by electron-phonon nor by magnetic interactions.

Although as far there is no affirmative experimental evidence for whether POS has spin-singlet or spin-triplet pairing, the mechanism and the symmetry of the superconducting pairing have been studied in many theoretical works and several candidates for the pairing potential were proposed. In reference [8] the author using phenomenological Ginzburg-Landau theory to discuss the two superconducting phases based on the cubic crystal symmetry T_h, where the gap function is considered for the spin-singlet pairing case. For the high temperature phase it is considered to be strongly anisotropic s-wave state, while for the low temperature phase it is considered to be anisotropic $s+id$-wave state. At present, however, the pairing symmetry of the superconducting energy gap, as well as whether the superconductivity is of spin singlet or spin triplet pairing, still remain unclear.

As we know tunnelling spectroscopy of superconductors is a useful tool and is widely used in probing the superconducting pairing symmetry and the local density of state (LDOS) [12]. For example, zero-bias conductance peak (ZBCP) in tunnelling spectroscopy is a clear signature of an anisotropic pairing in most unconventional

[a] e-mail: gysun@xmu.edu.cn

$$\int d\mathbf{r}' \begin{bmatrix} (H_0(\mathbf{r}') - \eta_s h(\mathbf{r}'))\delta(\mathbf{r}-\mathbf{r}') & \Delta_{s\overline{s}}(\mathbf{r},\mathbf{r}') \\ \Delta^{\star}_{\overline{s}s}(\mathbf{r},\mathbf{r}') & -(H_0(\mathbf{r}') + \eta_s h(\mathbf{r}'))\delta(\mathbf{r}-\mathbf{r}') \end{bmatrix} \begin{bmatrix} u_s(\mathbf{r}') \\ v_{\overline{s}}(\mathbf{r}') \end{bmatrix} = E \begin{bmatrix} u_s(\mathbf{r}) \\ v_{\overline{s}}(\mathbf{r}) \end{bmatrix} \quad (1)$$

superconductors, which is resulted from the fact that zero-energy states are formed due to the interference between incident and Andreev reflected quasiparticles, which may experience pair potentials of opposite signs when the pairing is anisotropic. Asano et al. have studied the tunnelling conductance of normal metal/insulator/POS junctions for both spin-singlet and spin-triplet pairing states [7]. They found that the conductance is sensitive to the relation between the direction of the electric current and the position of point nodes. Peak structures in the sub gap conductance were got for spin-triplet pairing of the energy gap, which show that POS may be a spin-triplet superconductor if sub-gap conductance peak is observed in future experiments. In the presence of exchange field, however, such as in ferromagnet/superconductor junctions, the transport of incident and Andreev reflected quasiparticles is spin-dependent, and as a result the properties of the Andreev reflection (AR) process, as well as the tunnelling conductance spectra, will be modified [12–17]. On the other hand, spin-dependent tunnelling in ferromagnet/superconductor junctions provides a possible way to determine the degree of spin polarization in the ferromagnet [18,19]. The purpose of the present paper is to study the spin-polarization effects on the tunnelling conductance spectra of ferromagnet/POS junctions, while only spin-singlet pairing potential of the POS is discussed. We will discuss the effects of spin polarization of the ferromagnet, the interface barrier, as well as the nodal structures of superconducting energy gap of the POS, on the tunnelling conductance spectra of such structures.

2 Model and formulation

The system under consideration is sketched in Figure 1a, a ferromagnet (FM) and a POS connect at $z = 0$, and the interface is assumed to be perfectly flat and is described by a δ-type barrier $V(\mathbf{r}) = V_0\delta(z)$, while $V_0 = 0$ and ∞ correspond to two limits of metallic and tunnel junctions, respectively. The FM is described by an effective single-particle Hamiltonian for spin-polarized electrons. Here we neglect the influence of the magnetization of the FM on the orbital motion of the conduction electron for it is much smaller than that via the exchange interaction. Our study is based on the Blonder-Tinkham-Klapwijk (BTK) theory [20], which was first extended to study spin-dependent electron transport in the case of FM/conventional superconductor junctions by Jong et al. [21] The behavior of quasiparticles in such structures is described by the Bogoliubov-de Gennes (BdG) equation [22,23]. In the absence of spin-flip scattering, the spin-dependent four-component BdG equation will be decoupled into two sets of (two-component) equations, one for the spin-up electron and spin-down hole quasiparticles ($u_\uparrow(\mathbf{r})$, $v_\downarrow(\mathbf{r})$), and the other for ($u_\downarrow(\mathbf{r})$, $v_\uparrow(\mathbf{r})$). The BdG equation for ($u_s(\mathbf{r}), v_{\overline{s}}(\mathbf{r})$) ($s =\uparrow$ or $\downarrow$) can be given as

see equation (1) above

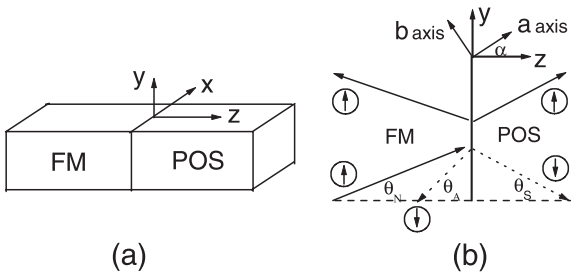

Fig. 1. Schematic illustrations of (a) FM/POS junction structures and (b) quasiparticle tunnelling processes in such structures.

where $H_0(\mathbf{r}) = -(\hbar^2/2m)\bigtriangledown^2 + V(\mathbf{r}) - E_F$, E is the quasiparticle energy relative to the Fermi energy level E_F. $\eta_s = 1$ for $s =\uparrow$ and -1 for $s =\downarrow$, while $\overline{s}$ denotes the opposite spin direction of s. In principle, owing to the interplay between them near the interface, the superconducting properties of the POS and the ferromagnetic properties of the FM should be determined in a self-consistent way. Here for simplicity we take both the pair potential of the POS and the exchange energy of the FM as step functions, $\Delta_{s\overline{s}}(\mathbf{R},\hat{\mathbf{k}}) = \Delta_{s\overline{s}}(\hat{\mathbf{k}})\Theta(z)$ and $h(\mathbf{R}) = h_0\Theta(-z)$, where $\Delta_{\overline{s}s}(\mathbf{R},\hat{\mathbf{k}})$ is the Fourier transformation of $\Delta_{\overline{s}s}(\mathbf{R},\mathbf{r}_r)$, with $\mathbf{R} = (\mathbf{r}+\mathbf{r}')/2$ and $\mathbf{r}_r = (\mathbf{r}-\mathbf{r}')$ are the center-of-mass and relative coordinates, respectively. $\Theta(z)$ is the unit step function. In the weak coupling theory, the superconducting pairing only occurs near the Fermi surface, so approximately the wavevector is fixed on the Fermi surface, i.e., $|\mathbf{k}| = k_F$, and $\hat{\mathbf{k}} = \mathbf{k_F}/k_F$ is a unit vector denotes the direction of the wave-vector, $\hat{\mathbf{k}} = (\cos\phi\sin\theta_S, \sin\phi\sin\theta_S, \cos\theta_S)$. The pair potential of spin-singlet superconductivity is given by

$$\Delta(\hat{\mathbf{k}}) = \Delta(\theta_S,\phi) = id(\hat{\mathbf{k}})\sigma_y \quad (2)$$

where σ_y is the Pauli matrix. Several candidates of pair potential are proposed for the spin-singlet superconductivity of the POS phenomenologically, which are compatible to the observed nodal structure [7,8]. One possible candidate is

$$d(\hat{\mathbf{k}})_1 = \begin{cases} \Delta_0\frac{3}{2}(1-\hat{k}_x^4-\hat{k}_y^4-\hat{k}_z^4) & \text{A phase} \\ \Delta_0(1-\hat{k}_y^4-\hat{k}_z^4) & \text{B phase} \end{cases} \quad (3)$$

with six ($[\pm 100], [0 \pm 10], [00 \pm 1]$) point nodes for A phase and four ($[0 \pm 10], [00 \pm 1]$) point nodes for B phase, respectively. Δ_0 is the amplitude of the pair potential at zero temperature. A second possible candidate is

$$d(\hat{\mathbf{k}})_2 = \begin{cases} \Delta_0(1-\hat{k}_x^4-\hat{k}_y^4) & \text{A phase} \\ \Delta_0(1-\hat{k}_y^4) & \text{B phase} \end{cases} \quad (4)$$

which is a nodal hybrid pair potential structure with four ($[\pm 100], [0 \pm 10]$) and two ($[0 \pm 10]$) point nodes, for A and B phase, respectively. The above two candidates belong

$$a_{\overline{s}s} = \frac{\kappa(k_z^s + q_z - 2iq_zZ)(k_z^{\overline{s}} - q_z - 2iq_zZ) - (k_z^s - q_z - 2iq_zZ)(k_z^{\overline{s}} + q_z - 2iq_zZ)}{D} \tag{15}$$

to the so-called anisotropic s-wave pairing state. Here it should be noted that it is not limited to the above candidates which can give rise to six (or four or two) point nodes. For example, a third candidate can be given as

$$d(\hat{\mathbf{k}})_3 = \begin{cases} \Delta_0(\hat{k}_x\hat{k}_y + \hat{k}_y\hat{k}_z + \hat{k}_z\hat{k}_x) & \text{A phase} \\ \Delta_0\left[\frac{3}{2}(1-\hat{k}_x^4-\hat{k}_y^4-\hat{k}_z^4)+i(\hat{k}_z^2-\hat{k}_x^2)\right] & \text{B phase} \end{cases} \tag{5}$$

where the A phase is a linear combination of three d-wave gap function which has six point nodes, and the B phase is an anisotropic $s+id$-wave pairing state with two point nodes on the Fermi surface in $[0 \pm 10]$ directions. The d-wave component of the B phase breaks the cubic crystal symmetry and the time reversal symmetry, and consequently it is expected that a spontaneous magnetization be observed by the μSR measurement [24].

Since translational invariance is satisfied in the interface plane, so the momentum parallel to the interface, $\mathbf{k}_\parallel = (k_x, k_y)$, is conserved, and the quasiparticle wave function can be written as

$$\begin{bmatrix} u_s(\mathbf{r}) \\ v_{\overline{s}}(\mathbf{r}) \end{bmatrix} = \psi^{\mathrm{FM(POS)}}(z)\exp(i\mathbf{k}_\parallel \cdot \mathbf{r}_\parallel) \tag{6}$$

with

$$\psi^{\mathrm{FM}}(z) = \begin{pmatrix} 1 \\ 0 \end{pmatrix} e^{ik_z^s z} + b_{ss}\begin{pmatrix} 1 \\ 0 \end{pmatrix} e^{-ik_z^s z} + a_{\overline{s}s}\begin{pmatrix} 0 \\ 1 \end{pmatrix} e^{ik_z^{\overline{s}} z} \tag{7}$$

for $z \le 0$,

$$\psi^{\mathrm{POS}}(z) = c_{ss}\begin{pmatrix} u_+ e^{i\phi_+/2} \\ v_+ e^{-i\phi_+/2} \end{pmatrix} e^{iq_z z} + d_{\overline{s}s}\begin{pmatrix} v_- e^{i\phi_-/2} \\ u_- e^{-i\phi_-/2} \end{pmatrix} e^{iq_z z} \tag{8}$$

for $z \ge 0$, where

$$\begin{aligned} k_z^s &\approx \sqrt{2m(E_F + \eta_s h_0)/\hbar^2}\cos\theta_N \\ k_z^{\overline{s}} &\approx \sqrt{2m(E_F + \eta_{\overline{s}} h_0)/\hbar^2}\cos\theta_A \\ q_z &\approx \sqrt{2mE_F/\hbar^2}\cos\theta_S \end{aligned} \tag{9}$$

are z-component wavevectors of electrons and holes in the FM, and that of quasiparticles in the POS, with θ_N, θ_A, θ_S are injection and Andreev reflection angles in the FM, and transmission angle in the POS, respectively, as shown in Figure 1b. Here it is assumed that the effective mass of quasiparticles and the Fermi energy in the FM are equal to those in the POS. And

$$\begin{aligned} u_\pm^2 &= \frac{1}{2}\left[1 + \sqrt{1 - |d(\hat{\mathbf{k}}_\parallel, \pm\hat{k}_z)|^2/E^2}\right] \\ v_\pm^2 &= \frac{1}{2}\left[1 - \sqrt{1 - |d(\hat{\mathbf{k}}_\parallel, \pm\hat{k}_z)|^2/E^2}\right] \end{aligned} \tag{10}$$

where $d(\hat{\mathbf{k}}_\parallel, \pm\hat{k}_z) = d(\hat{\mathbf{k}}_\parallel(\theta_{S\pm}, \phi), \pm\hat{k}_z(\theta_{S\pm}, \phi))$, which is given by equations (3–5), with $\theta_{S\pm} = \theta_S \mp \alpha$, α is the angle between the z-axis and the a-axis of the crystal, as shown in Figure 1b, and

$$\phi_\pm = \cos^{-1}\left[\frac{d(\hat{\mathbf{k}}_\parallel, \pm\hat{k}_z)}{|d(\hat{\mathbf{k}}_\parallel, \pm\hat{k}_z)|}\right] \tag{11}$$

are phases of the effective pair potentials experience by the electron-like quasiparticles (ELQ) and hole-like quasiparticles (HLQ) in the POS, respectively.

In the FM, wave vectors of electrons with different spin direction, k_F^s and $k_F^{\overline{s}}$, are not equal due to the presence of the ferromagnetic exchange energy h_0. Also, neither of them is equal to that of the POS, k_F. As we have pointed out that the wave-vector components parallel to the interface are assumed to remain unchanged in the reflection and transmission processes, i.e., they must satisfy the condition: $k_F^s \sin\theta_N = k_F^{\overline{s}} \sin\theta_A = k_F \sin\theta_S$. As a result, θ_N, θ_A, and θ_S differs from each other except when θ_N equals zero. For example, since $k_F^\uparrow > k_F > k_F^\downarrow$, we have $\theta_N < \theta_S < \theta_A$ for the incident electrons with spin up, as sketched in Figure 1b. In this case, a virtual Andreev reflection process will occur if $\theta_N > \sin^{-1}(k_F^\downarrow/k_F^\uparrow)$, therefore the z-component of the wavevector in the Andreev reflection process becomes purely imaginary and as a result the Andreev-reflected quasiparticles do not propagate. Furthermore, the z-component of the wavevector in either ELQ or HLQ transmission also becomes purely imaginary when $\theta_N > \sin^{-1}(k_F/k_F^\uparrow)$, and as a result a total reflection occurs and the net current from the FM to the POS vanishes. There is an opposite result, $\theta_N < \theta_S < \theta_A$, for the incident electrons with spin down. In this case, neither virtual AR nor total reflection processes can take place. By matching the boundary conditions at $z = 0$ [20]

$$\Psi^{\mathrm{FM}}(z=0) = \Psi^{\mathrm{POS}}(z=0) \tag{12}$$

$$\frac{d\Psi^{\mathrm{POS}}(\mathbf{r})}{dz}|_{z=0} - \frac{d\Psi^{\mathrm{FM}}(\mathbf{r})}{dz}|_{z=0} = \frac{2mV_0}{\hbar^2}\Psi^{FM}|_{z=0} \tag{13}$$

we obtain the coefficients of the normal reflection b_{ss} and the Andreev reflection $a_{\overline{s}s}$ as

$$b_{ss} = \frac{2k_z^s(v_+/u_-)(q_z + q_z)e^{-i\phi_+}}{D} \tag{14}$$

see equation (15) above

where $D = \kappa(k_z^s - q_z + 2iq_zZ)(k_z^{\overline{s}} - q_z - 2iq_zZ) - (k_z^s + q_z + 2iq_zZ)(k_z^{\overline{s}} + q_z - 2iq_zZ)$, $\kappa = v_+v_-\exp[-i(\phi_+ - \phi_-)]/u_+u_-$, $Z = Z_0/\cos\theta_S$ with $Z_0 = 2mV_0/\hbar^2k_F$ is a dimensionless parameter describing barrier strength of the interface. The tunnelling conductance of the junctions can be obtained by extending the BTK formula to include the effects of spin-dependent transport. For spin-s electrons incident we got

$$\hat{G}_s = \mathrm{Re}\left[1 + \frac{\mathrm{k}_\mathrm{z}^{\overline{\mathrm{s}}}}{\mathrm{k}_\mathrm{z}^{\mathrm{s}}}|\mathrm{a}_{\overline{\mathrm{s}}\mathrm{s}}|^2 - |\mathrm{b}_{\mathrm{ss}}|^2\right] \tag{16}$$

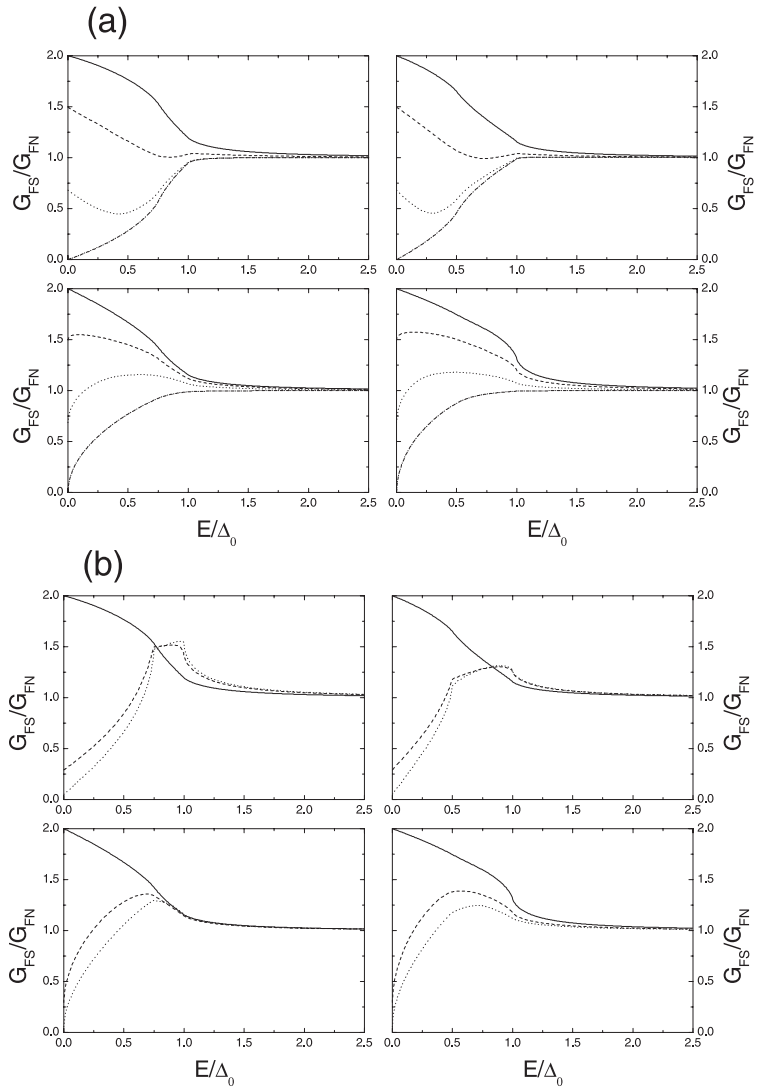

Fig. 2. Normalized tunnelling conductance of FM/POS junctions as a function of the quasiparticle energy, E/Δ_0. Pair potential of the POS is $d(\hat{\mathbf{k}})_1$. (a) For different values of P, $P = 0$ (solid), 0.5 (dash), 0.8 (dot), 0.999 (dot dash), respectively, with $Z_0 = 0$. (b) For different values of Z_0, $Z_0 = 0$ (solid), 2 (dash), 5 (dot), with $P = 0$. In both (a) and (b), the left and the right columns correspond to the high temperature and low temperature phases, while the upper and low panel correspond to $\alpha = 0$ and $\alpha = \pi/4$, respectively.

The total conductance is given by

$$G = \int_0^{2\pi} d\phi \int_0^{\pi/2} d\theta_N \sin\theta_N \left[\hat{G}_\uparrow k_{Fz}^\uparrow \frac{1+P}{2} + \hat{G}_\downarrow k_{Fz}^\downarrow \frac{1-P}{2} \right] \quad (17)$$

where $P = h_0/E_F$ is the spin polarization rate of the FM. Here we should define a normalization factor of the conductance, G_N, which is just given by the above equation with the POS be replaced by a normal metal, i.e., $\Delta(\hat{\mathbf{k}}) = 0$.

3 Results and discussion

In Figure 2a, we plot the tunnelling conductance spectra of FM/POS junctions as a function of the quasiparticle energy E, with pair potential of the POS given by $d(\hat{\mathbf{k}})_1$, for different values of the spin-polarization rate P of the FM. The interface barrier strength is taken to be zero, $Z_0 = 0$, which corresponds to the case of a metallic junction. The conductance is normalized by that when the POS is replaced by a normal metal. The left and right columns correspond to the high temperature and low temperature phases, while the upper and low panel correspond to $\alpha = 0$ and $\alpha = \pi/4$, respectively. We note that there are three node directions, say, $x-$, $y-$, $z-$directions, respectively, for the high temperature phase of $d(\hat{\mathbf{k}})_1$, while there are two node directions, say, $y-$ and $z-$directions, for the low temperature phase of $d(\hat{\mathbf{k}})_1$. First, it is found that the subgap conductance is suppressed with increasing of the spin-polarization rate P for all cases. Especially, the zero-bias conductance is suppressed from 2 (which is known as ZBCP, resulting from Andreev reflection of the tunneling electrons) for $P = 0$ to 0 (disappearing of ZBCP) for $P = 0.999$, where $P = 0$ and 0.999 correspond to the FM of normal metal and nearly half-metallic ferromagnet cases, respectively. The suppression of the subgap

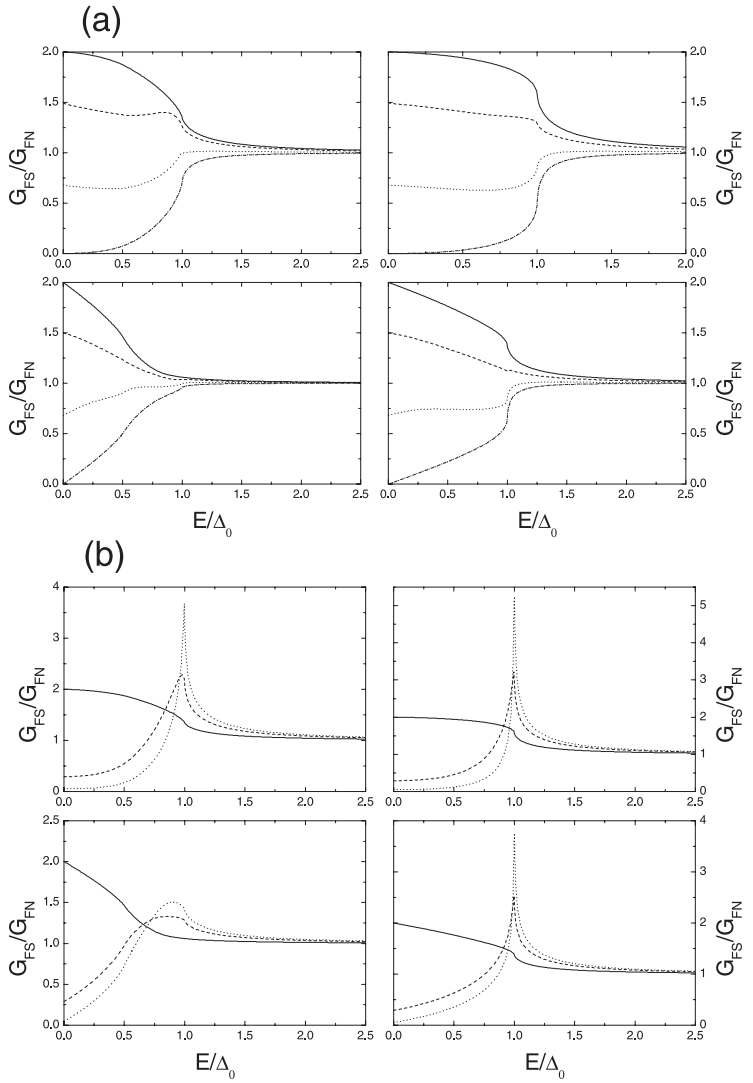

Fig. 3. The same as in Figure 2, except for the pair potential of the POS is given by $d(\hat{\mathbf{k}})_2$.

conductance is resulted from suppression of the Andreev reflection process with increasing of P. As is known that the ferromagnetic exchange energy gives rise to the mismatch between the wavevectors of spin-up and spin-down quasiparticles, which, is just the reason that leads to the suppression of the AR process, and the larger mismatch between the wavevectors of different spins (the larger P), the much suppression of the AR process will be got, until the AR is totally suppressed for the half-metallic ferromagnet neighboring case. On the other hand, the quantitative suppression of zero-bias conductance may be used to deduce the spin-polarization rate of the neighboring FM, from experimental viewpoint [25–27]. Secondly, the residual conductances within the energy gap, as well as their different energy-dependent behaviors between the upper ($\alpha = 0$) and low ($\alpha = \pi/4$) panels, giving information on the anisotropic pairing property of the superconducting energy gap of the POS, which may be used as comparison for experimental results. In Figure 2b, plotting are the tunnelling conductance spectra for a variety of values of the interface barrier strength Z_0, with $P = 0$ taken. Here, it is found that the subgap conductance is suppressed with increasing of Z_0, which, in effect increases the mismatch between the wavevectors of quasiparticles with different spin directions, and consequently leads to the suppression of the AR process, too. On the other hand, we note that the decreasing behaviors of the zero-bias conductance are different: it is decreasing but remaining a peak shape with the increasing of P in the up panel of Figure 2a, while it is decreasing and actually developing into a dip shape in the low panel of Figure 2a and in Figure 2b, where the later is called zero-bias conductance splitting [12], which may be a signature of an opening gap of the POS. Moreover, it is also found that for both high and low temperature phases of $d(\hat{\mathbf{k}})_1$, the tunnelling conductance spectra have the same zero-bias values for same P, while they are different in the energy gap associating with different anisotropic pairing symmetries of the POS. Parts of the results of reference [7] are reproduced.

In Figures 3a(b) and 4a(b), we plot parallel results as in Figures 2a(b), for pair potentials of the POS given by $d(\hat{\mathbf{k}})_2$ and $d(\hat{\mathbf{k}})_3$, respectively. It is found that the main features of the P and Z_0 dependence of the tunnelling

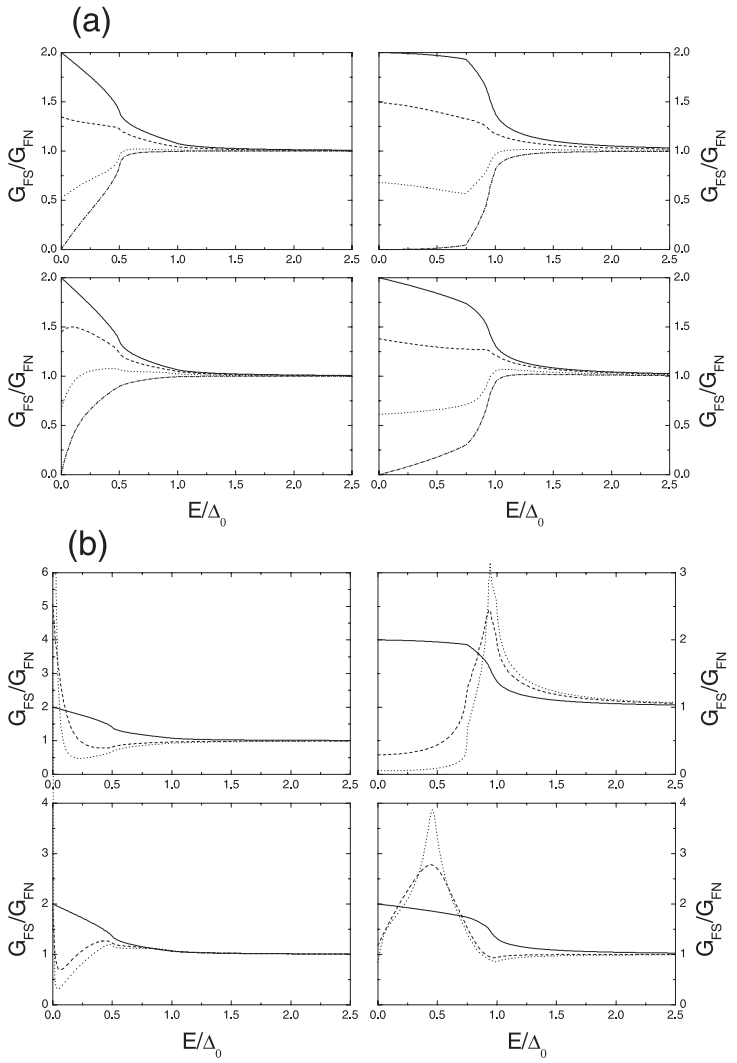

Fig. 4. The same as in Figure 2, except for the pair potential of the POS is given by $d(\hat{\mathbf{k}})_3$.

conductance remain as in Figures 2a(b): increasing P or Z_0 will lead to suppression of the sub-gap conductance, under the same physical explanation. However, the line shapes of the sub-gap conductance spectra are different, indicating different anisotropic pairing properties, as well as different nodal structures, of the pair potentials. For example, for the high temperature phase of $d(\hat{\mathbf{k}})_2$, there are two node directions, say, x and y-directions, and therefore four point nodes on the Fermi surface, while there are only one node direction and two point nodes for the corresponding low temperature phase. So it is much anisotropic for the pair potential of high temperature phase than that of low temperature one. In the upper panel of Figure 3a, where $\alpha = 0$, it is found that the sub-gap conductance is fairly flat with increasing of E/Δ_0, while it develops into a U line shape for larger P ($P = 0.8$ and 0.999). However, in the low panel of Figure 3a, where $\alpha = \pi/4$, the sub-gap conductance becomes much sloping, and turns into a V line shape for $P = 0.999$. Moreover, we find that it is much sloping for the conductances in left column than those in the right column, indicating the much anisotropic for the pair potential of high temperature phase than that of the low temperature one. In the upper panel of Figure 3b, a large enhancement of the conductance occurs at $E/\Delta_0 = 1$ with increasing of the barrier strength Z_0, at the same time it is largely suppressed to a U line shape inside the sub-gap. However, in the low panel where $\alpha = \pi/4$, the conductance is only damply enhanced at $E/\Delta_0 = 1$ and is suppressed to a V line shape inside the sub-gap with increasing Z_0 for the high temperature phase (low-left), while for the low temperature phase (low-right) it is only slightly flopped inside the sub-gap, and the peak height at $E/\Delta_0 = 1$ is slightly reduced, with respect to the case of $\alpha = 0$ for the low temperature phase (up-right).

For pair potential candidate of $d(\hat{\mathbf{k}})_3$ given by equation (5), as stated above, its high temperature phase is a linear combination of three d-wave gap functions, which is of cubic symmetry with six point nodes and is highly anisotropic, while the low temperature phase is an anisotropic $s+id$-wave pair potential with two point nodes in y-direction. In the left column of Figure 4a, it is found that the tunnelling conductance is suppressed to a V shape

for $E/\Delta_0 < 0.5$ with increasing P, and has a inflexion at $E/\Delta_0 = 0.5$. For the low temperature phase in the right column, the sub-gap conductance is fairly flat with increasing of E/Δ_0 and is suppressed to a U line shape with increasing P. For the case of different interface barrier strength Z_0 in Figure 4b, in the left column first, it is found that the zero-bias conductance is largely enhanced, i.e., ZBCP occurs, with increasing of Z_0, indicating the formation of bound states at $E = 0$. Again, a inflexion occurs at $E/\Delta_0 = 0.5$. For the low temperature phase with $\alpha = 0$, as shown in the upper-right of Figure 4b, the sub-gap conductance is suppressed to a U shape and a peak occurs at $E/\Delta_0 = 1$, with increasing of Z_0. While in the low-right of Figure 4b, the conductance is generally suppressed except a peak occurs at about $E/\Delta_0 = 0.5$, with increasing of Z_0, indicating the formation of bound states inside the sub-gap. The nearly vanishing conductance at about $E/\Delta_0 < 0.75$ for $Z_0 = 5$ (or $P = 0.999$), of the low temperature phase of $d(\hat{\mathbf{k}})_3$ with $\alpha = 0$, is consistent with reference [7].

4 Summary

In summary, we have theoretically studied the tunnelling conductance spectra of FM/POS junctions, where FM is a ferromagnetic metal described by an effective single-particle Hamiltonian for spin-polarized electrons, while POS is the recently found nonmagnetic and heavy fermion unconventional superconductor, whose superconductivity is described by three possible candidates of pairing symmetry of the superconducting energy gap. We have discussed the spin-polarization effects on the tunnelling conductance spectra, with respect to different strength of ferromagnetism of the FM and different strength of the interface barrier. Different features of the tunnelling conductance spectra were got, which may serve as useful theoretical comparisons for future experiments.

This work is supported by the National Science Foundation of China (Grant No. 10225420).

References

1. E.D. Bauer, N.A. Frederick, P.-C. Ho, V.S. Zapf, M.B. Maple, Phys. Rev. B **65**, 100506(R) (2002)
2. R. Vollmer, A. Faisst, C. Pfleiderer, H.v. Lohneysen, E.D. Bauer, P.-C. Ho, V.S. Zapf, M.B. Maple, Phys. Rev. Lett. **90**, 057001 (2003)
3. N. Oeschler, P. Gegenwart, F. Steglich, N.A. Frederick, E.D. Bauer, M.B. Maple, Acta Phys. Pol. B **34**, 959 (2003)
4. K. Izawa, Y. Nakajima, J. Goryo, Y. Matsuda, S. Osaki, H. Sugawara, H. Sato, P. Thalmeier, K. Maki, Phys. Rev. Lett. **90**, 117001 (2003)
5. M.B. Maple, P.-C. Ho, V.S. Zapf, N.A. Frederick, E.D. Bauer, W.M. Yuhasz, F.M. Woodward, J.W. Lynn, J. Phys. Soc. Jpn **71** (Suppl.), 23 (2002)
6. H. Kotegawa, M. Yogi, Y. Imamura, Y. Kawasaki, G.-q. Zheng, Y. Kitaoka, S. Ohsaki, H. Sugawara, Y. Aoki, H. Sato, Phys. Rev. Lett. **90**, 027001 (2003)
7. Y. Asano, Y. Tanaka, Y. Matsuda, S. Kashiwaya, Phys. Rev. B **68**, 184506 (2003)
8. Jun Goryo, Phys. Rev. B **67**, 184511 (2003)
9. K. Maki, P. Thalmeier, Q. Yuan, K. Izawa, Y. Matsuda, `cond-mat/0212090`
10. Y. Aoki, T. Namiki, S. Osaki, S.R. Saha, H. Sugawara, H. Sato, J. Phys. Soc. Jpn **71**, 2098 (2002)
11. D.L. Cox, A. Zawadowski, Adv. Phys. **47**, 599 (1998)
12. S. Kashiwaya, Y. Tanaka, Rep. Prog. Phys. **63**, 1641 (2000)
13. Y. Tanaka, S. Kashiwaya, Phys. Rev. Lett. **74**, 3451 (1995)
14. S. Kashiwaya, Y. Tanaka, N. Yoshida, M.R. Beasley, Phys. Rev. B **60**, 3572 (1999)
15. J.X. Zhu, B. Friedman, C.S. Ting, Phys. Rev. B **59**, 9558 (1999)
16. I. Zutic, O.T. Valls, Phys. Rev. B **60**, 6320 (1999)
17. A.A. Golubov, Physica C **46**, 326 (1999)
18. I.I. Mazin, Phys. Rev. Lett. **83**, 1427 (1999)
19. I.I. Mazin, A.A. Golubov, B. Nadgorny, J. Appl. Phys. **89**, 7576 (2001)
20. G.E. Blonder, M. Tinkham, T.M. Klapwijk, Phys. Rev. B **25**, 4515 (1982)
21. M.J.M. de Jong, C.W.J. Beenakker, Phys. Rev. Lett. **74**, 1657 (1995)
22. P.G. de Gennes, *Superconductivity of Metals and Alloys* (Benjamin, New York, 1996)
23. C. Bruder, Phys. Rev. B **41**, 4017 (1990)
24. D.E. MacLaughlin, J.E. Sonier, R.H. Heffner, O.O. Bernal, Ben-Li Young, M.S. Rose, G.D. Morris, E.D. Bauer, T.D. Do, M.B. Maple, Phys. Rev. Lett. **89**, 157001 (2002)
25. R.J. Soulen Jr., J.M. Byers, M.S. Osofsky, B. Nadgorny, T. Ambrose, S.F. Cheng, P.R. Broussard, C.T. Tanaka, J. Nowak, J.S. Moodera, A. Barry, J.M.D. Coey, Science **282**, 85 (1998)
26. R.J. Soulen, Jr., M.S. Osofsky, B. Nadgorny, T. Ambrose, P. Broussard, S.F. Cheng, J. Byers, C.T. Tanaka, J. Nowack, J. S. Moodera, G. Laprade, A. Barry, M.D. Coey, J. Appl. Phys. **85**, 4589 (1999)
27. S.K. Upadhyay, A. Palanisami, R.N. Louie, R.A. Buhrman, Phys. Rev. Lett. **81**, 3247 (1998)